
THE FINITE ELEMENT ANALYSIS OF A TIDAL TURBINE

Miriam Said

Student Number: 1673667



Declaration:

I hereby declare:

That except where reference has clearly been made to work by others, all the work presented in this report is my own work;

That it has not previously been submitted for assessment; and

That I have not knowingly allowed any of it to be copied by another student.

I understand that deceiving or attempting to deceive examiners by passing off the work of another as my own is plagiarism. I also understand that plagiarising the work of another or knowingly allowing another student to plagiarise from my work is against the University regulations and that doing so will result in loss of marks and possible disciplinary proceedings against me.

Signed Miriam Said

Date 29th March 2019

,

List of Figures

Figure 1 - Primary energy by fuel (Bp, 2018)	1
Figure 2 – HS300 HATT (Lynn 2013)	5
Figure 3 - HS1000 (Lynn 2013)	5
Figure 4 - SeaGen Manufactured by Marine Current Turbines.....	7
Figure 5 - Atlantis Resources AR1500.....	8
Figure 6 - Open Hydro (Lynn 2013)	9
Figure 7 - SR2000 (ORBITAL MARINE POWER 2018)	10
Figure 8 - Spar support structure.....	11
Figure 9 – Example of carbon fibre tidal turbine blade (2018)	14
Figure 10 - Wortmann FX63-137 aerofoil (Ellis et al. 2018)	17
Figure 11 - Turbine rotor (Ellis et al. 2018)	17
Figure 12 - Blade Geometry (Ellis et al. 2018)	17
Figure 13 - Ansys Workbench, Static Structural.....	18
Figure 14 - CFD pressure extraction.....	19
Figure 15 - CFD pressure extraction.....	19
Figure 16 - Composite Material process in ANSYS Workbench.....	20
Figure 17 - ACP Toolbar.....	20
Figure 18 - Stackups dialog box.....	21
Figure 19 - Generated Ply thicknesses.....	21
Figure 20 - Failure criteria dialog box.....	22
Figure 21 - Final blade analysis process in ANSYS workbench.....	22
Figure 23 - CFD Pressure distributions.....	23
Figure 24 - Mesh Sensitivity study results (No. of Nodes against Deformation of blade)	24
Figure 25 - Generated blade mesh.....	25
Figure 26 - Composite blade Mesh.....	26
Figure 27 - Flow chart of design process.....	27
Figure 28 - Solid Blade.....	28
Figure 29 - Hollow blade.....	28
Figure 30 - Safety factor for hollow blade.....	29
Figure 31 - Cross Section view of spar support structure.....	29
Figure 32 – Aluminium blade with spars.....	30
Figure 33 – Summarised Aluminium blade results.....	30
Figure 34 – CFRP blade (1 mm Shear Webs)	31
Figure 35 – CFRP blade (0.5 mm Shear Webs)	31
Figure 36 – GFRP blade (0.5 mm Shear Webs)	32
Figure 37 – Cross beam spar support structure	32
Figure 38 – Tsai -Wu comparison between GFRP (left) and GFRP cross webs (right).....	33
Figure 39 – Composite blade comparison.....	33
Figure 40 – CFRP (top) vs GFRP (bottom).....	34
Figure 41 – Comparison between composite blade layups of CFRP blade.....	35
Figure 42 – Failure comparison between the composite layups.....	36
Figure 43 – Upscaled blades comparison.....	37
Figure 44 – Final CFRP blade.....	37

List of Tables

Table 1 - Andritz Hydro Hammerfest, HS1000 design parameters.....	5
Table 2 - Comparison between SeaGen S and SeaGen U (MCT 2013).....	7
Table 3 - AR1500 HATT design parameters (SIMEC Atlantis Energy 2015).....	8
Table 4 – Open Hydro design parameters (Gov.je, 2019) (Lynn 2013).....	9
Table 5 – SR2000 design parameters.....	10
Table 6 - Composite Material Comparison.....	12
Table 7 - Composite Layup 1.....	13
Table 8 - Composite Layup 2.....	13
Table 9 - Mesh sensitivity study results.....	24
Table 10 - Mesh details.....	25
Table 11 - Composite blade mesh details	26
Table 12 - Upscaled Aluminium blades.....	34
Table 13 – Modal Results from Blade Simulations	43
Table 14 - Inverse Reserve factors of Failure Criteria for Composite Blades.....	43

Nomenclature

HATT	-	Horizontal Axis Tidal turbine
FEA	-	Finite Element Analysis
CFD	-	Computational Fluid Dynamics
CFRP	-	Carbon Fibre Reinforced Polymer
GFRP	-	Glass Fibre Reinforced Polymer
IRF	-	Inverse Reserve Factor

ACKNOWLEDGMENTS

I would like to express my sincere gratitude to my supervisors, Professor Tim O'Doherty and Dr. Allan Mason Jones for their constant support throughout the duration of this project. I would also like to thank Robert Ellis for his assistance and for providing me with the CFD data that allowed me to proceed with my simulations. Finally, I would also like to thank Robynne Murray for providing me with valuable information concerning current composite tidal turbine blades.

ABSTRACT

Tidal turbines are growing technologies that are utilised within the renewable energy sector. Limited research has led to the comparison with wind turbine concepts to validate further understanding, but with water being 832 times denser than air, it has potential to exceed current output from wind turbines. The aim of this project was to enhance the internal blade design of a Horizontal Axis Tidal Turbine (HATT) on the basis of process variables such as material selection, internal structure and composite layup. The materials of interest included Aluminium, Carbon Fibre Reinforced Polymers (CFRP) and Glass Fibre Reinforced Polymers (GFRP). Different spar support structures were explored, and a suitable design was identified. This design used Finite Element Analysis (FEA) to analyse the blade with the selected materials and various composite layups, this resulted in a blade model capable of withstanding the high loads exerted by the marine environment. The design process confirmed the suitability of using CFRP over GFRP, as CFRP exhibited considerably lower stresses and deformations. The final CFRP blade comprised a box spar support structure and a refined composite layup. This model found an 82% weight reduction in comparison to a solid aluminium blade whilst exhibiting acceptable modal responses.

TABLE OF CONTENTS

1	<i>Introduction</i>	1
2	<i>Literature review</i>	2
2.1	Marine Energy	2
2.2	Tidal current turbines	4
2.2.1	Andritz Hydro Hammerfest	5
2.2.2	Marine Current Turbines – SeaGen	6
2.2.3	Atlantis Resources	8
2.2.4	Open Hydro	9
2.2.5	Orbital Marine Power Limited	10
2.3	Blade design	11
2.4	Composites	12
2.5	Composite Material Selection	13
2.6	Composite failure criteria	15
3	<i>Methodology</i>	16
3.1	Design specifications	16
3.2	Solid Works	17
3.3	Finite Element Analysis	18
3.3.1	Modelling Composite Materials	20
3.4	CFD data	23
3.5	Mesh Generation	24
3.5.1	Mesh sensitivity study	24
3.5.2	Mesh details	25

3.5.3 Composite blade mesh details	26
3.6 Blade Design Process	27
4 Results & Discussion.....	27
4.1 Aluminium blade	28
4.1.1 Solid Blade	28
4.1.2 Hollow Blade	28
4.1.3 Optimised blade	29
4.2 Composite blade optimisation.....	31
4.2.1 CFRP Blade	31
4.2.2 GFRP Blade	32
4.3 Upscaled Blade optimisation	34
4.3.1 Composite Layup 1	35
4.3.2 Composite Layup 2	35
5 Conclusion	38
6 References	40
7 Appendices	43
7.1 Raw Data	43
7.2 Record of meetings.....	44

1 INTRODUCTION

The majority of energy produced in today's world results from the combustion of fossil fuels; summing to 85% of global energy production (Bp, 2018). The large consumption of these fuels results in a substantial release of CO₂ into the atmosphere, contributing further to current environmental issues such as climate change and global warming. Alongside the destructive side effects, the consumption of fossil fuels cannot persist due to the depletion in fuel reserves (Jenkins and Ekanayake 2018). To meet sustainable demands such as the IEA's 'Sustainable Development Scenario' for the reduction of carbon emissions to 50% by 2040, developments have progressed the nuclear, hydro and renewables sectors that account for the remaining 15% of global energy. The sector of increasing interest is the renewable energy sector, which continues to grow at a rate of 7% per annum, making it the fastest growing source of energy to date. (Bp, 2018) The increasing consumption of energy from renewables is illustrated in Figure 1, which displays the breakdown of primary energy. (Bp, 2018)

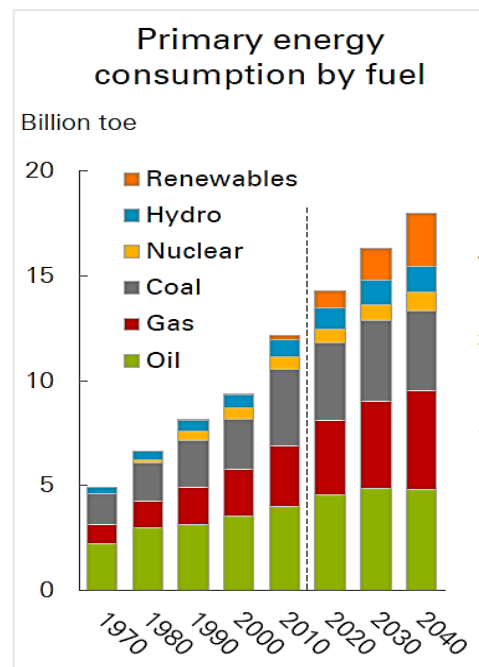


Figure 1 - Primary energy by fuel (Bp, 2018)

Within the category of renewable energies, the largest proportion consists of the wind and solar sectors, with a minority being attained from marine applications. New research seeks the development of marine energy technologies in order to accommodate the earth's growing energy demands.

The current project aims to facilitate this demand within the marine energy sector by improving current horizontal-axis tidal stream turbine rotor blades. Research on current wind turbine blades are used in the design of the key interior and surface configuration for tidal turbine blades. This report describes the process of enhancing a tidal stream turbine blade model.

Throughout the design process, the process variables involved a combination of blade structure, material selection, and composite layup to ensure that the blades are suitable to operate in the marine environment, thus overcoming any obstacles imposed by the harsh waters. Pressures were extracted for each iteration from previous Computational Fluid Dynamics data in order to simulate the hydrodynamic loads acting on the blade, resulting in modal responses that were further analysed. The analysis aided in the development of a surface mesh capable of modelling composite materials and a spar support structure based on beam elements. The final result will produce an FEA model capable of modelling the response of a tidal turbine blade to previously derived hydrodynamic loading.

2 LITERATURE REVIEW

2.1 Marine Energy

The oceans cover more than 70% of the earth's surface; validating the potential to use tides and waves in the generation of power (Jenkins and Ekanayake 2018). Within the marine environment, energy can be extracted in various ways; ocean wave, tidal range, tidal current, ocean current, ocean thermal energy, and salinity gradients. (OES, 2018)

The methods of interest include tidal stream generation (tidal range) and tidal current power. Tidal stream generation works on the basis of the gravitational pull from the moon and sun together with the rotation of the earth, resulting in a change in height of the earth's oceans. This variation in water height creates a long period wave, moving across the ocean. Thus, when the tidal wave reaches land it creates the variation in height of the water that is the tidal range (Jenkins and Ekanayake 2018). Tidal turbines utilise the kinetic energy of tidal currents to extract energy; similar with respect to wind turbines that instead use wind motion. Tidal turbines can be categorised into different subdivisions, the most common being horizontal axis tidal current turbines (HATT) and vertical axis tidal current turbines (VATT). Horizontal axis tidal current turbine blades rotate about a horizontal axis and are parallel to the direction of the

flow of water whereas vertical axis tidal current turbine blades rotate about a vertical axis and are perpendicular the direction of flow of the water. (Rourke et al. 2010) All categories of a tidal turbines consist of a rotor (number of blades mounted on a hub), a gearbox and a generator. The basic principle of a tidal turbine comprises the turning of the generator due to the flowing water pushing the rotor blades causing it to rotate, where the rotor and the generator are connected via a gearbox. The gearbox is used to convert the rotational speed of the rotor to the desired output speed of the generator shaft. The electricity generated is transmitted to land through the cables. (Rourke et al. 2010)

Many advantages arise from the use of tidal turbines; one of the advantages is the ease of predicting tidal cycles as tides are coupled relative to the movement of the earth, moon and sun, whereas other renewable energy sources such as wind energy are dependent on seasonal and short-term weather conditions. (Orbital Marine Power 2018) Predictable outputs of tidal energy suggests it is advantageous over other renewable sources as they offer a possibility of dispatchable power over randomly generated energy produced by the wind, wave and solar industries. (MCT 2012) As well as the predictability of ocean tides, the high-water density of the ocean also favours tidal energy over other renewables, offering a density of approximately 832 times larger than that of air. (Marsh 2004) Tidal turbines exert minor environmental impacts, where tidal turbines widely contradict some presumed environmental concerns, some of these concerns include:

Threat to marine wildlife (impact of turbine rotors): Due to the low operating speeds of tidal turbines, this concern can be considered negligible, especially when comparing turbine rotors to other devices that operate in the ocean such as boat propellers, which operate at much higher speeds. Therefore, tidal turbines are less likely to cause threat to marine wildlife compared to other ocean operations. (MCT 2012)

Pollution: As mentioned previously, renewable energy is a substitute to conventional renewable energy such as fossil fuels; thus, the tidal turbine industry will in fact aid in pollution reduction as a whole. (MCT 2012)

Conflicts with other sea users: Tidal turbines are constrained to only operate at locations with unusually high current velocities, these locations tend to be in areas, such as coastlines that are populated with rocky surfaces and are too dangerous for other sea operations, and hence sea users avoid such areas. (MCT 2012)

However, complications arise in the tidal energy sector, with the main issues being the high environmental loading on the turbine structure. This means that the structure must be durable enough to withstand such high loads. Accompanied with the large hydrodynamic loads, the high salt concentration in the ocean waters can lead to substantial corrosion to a turbine structure. Consequently, tidal turbines must comprise of corrosive resistant materials, which in large-scale cases can be very costly.

The main limitation of tidal turbines when compared to other renewable energy sources is the siting requirements. Tidal turbine locations usually require a mean spring peak tidal current speed greater than 2 - 2.5 m / s (Fraenkel 2007). If this criterion is not met, the design is not economically feasible, as it will result in an inadequate energy density. Thus, the tidal turbine industry is restricted in operating in various locations, as the sites that can provide these requirements for current speed are scarce in nature. (MCT 2012)

2.2 Tidal current turbines

The tidal energy industry is an emerging market nonetheless still in its early stages. Currently there are only a few operating tidal turbines in world, and some advanced prototypes that are currently being tested. The following section will describe the current status of tidal turbines in today's world.

The following listed turbines also demonstrate the similarity between the wind turbines and the tidal turbines; allowing wind engineering to be considered throughout the design process of a HATT.

2.2.1 Andritz Hydro Hammerfest

The Norwegian company Hammerfest storm was established in 1977 and created its first tidal stream turbine, the HS300 in 2003. The HS300 was installed in Kvasaland, 30km outside Hammerfest. (Lynn 2013) This device was considered to be the smaller case device and its success led to the development of the full-scale prototype, the HS100 illustrated in Figure 2.



Figure 2 – HS300 HATT (Lynn 2013)



Figure 3 - HS1000 (Lynn 2013)

(Gov.je, 2019) Both the HS300 and the HS100 consist of three blades mounted on a steel substructure that are anchored to the sea floor. The asymmetric blade design is pitched though 280° to optimize blade operation throughout the range of tidal current speeds. (Lynn 2013) The most recent turbine, the HS1000, has the following design parameters in Table 1:

Table 1 - Andritz Hydro Hammerfest, HS1000 design parameters

Parameters	
Blade length	9 m
Rotor Diameter	21 m
Rated Power	50-2000 kW (site dependent)
Operation Depth	35 – 100 m
Nacelle weight	130
Substructure weight	Approx. 150 tones
Service	Every 5 years
Lifetime	25 years

2.2.2 Marine Current Turbines – SeaGen

Marine Current Turbines (MCT) deployed the first offshore marine device on the world. The 300 kW device was installed in 2003, off the Lynmouth coast in Devon, England. The device operated for three years and then faced complete removal from the site in 2009; (Lynn 2013) The Company then introduced its next design known as SeaGen. SeaGen was deployed in 2008 by MCT, a Bristol based company. (Lynn 2013) The HATT turbine had an overall power output of 1.2MW. The turbine was considered to be the “world’s first utility-scale tidal stream turbine, in fast-flowing waters” located on the coast of Northern Ireland. SeaGen consists of some of the following design features:

- Two bladed HATT (Lynn 2013)
- Rotor located close to ocean surface, where tidal flows are the strongest deducing that 75% of energy is extracted at top of water column (MCT 2013)
- Advanced blade design techniques similar to those used for wind turbines produce fully optimised, asymmetrical, blade profiles.
- Safe and low maintenance due to the ease raising rotors and power units out of the water (MCT 2013)
- All power conditioning equipment are housed within the support structure and the electricity transmitted to shore is fully grid-compliant. (Lynn 2013)
- The 180° pitch-controlled rotor blades maximize energy capture therefore improving SeaGen’s power-generating capabilities (MCT 2013)

MCT offer two versions of SeaGen; SeaGen S, and SeaGen U. The differences between these versions are described in Table 2.

Table 2 - Comparison between SeaGen S and SeaGen U (MCT 2013)

Parameters	SeaGen S	SeaGen U
Rotor Diameter	16 – 20 m	16 – 20 m
Number of Turbine rotors	2	3
Rated Power	1.2-2MW @ 2.4 m/s	1.8-3MW @ 2.4 m/s
Water depth	24-40	22-50
Energy capture at 40% capacity factor lifetime	4,200 – 7,000 MWh/yr	6,300 – 10,000 MWh/yr
		20 years



Figure 4 - SeaGen Manufactured by Marine Current Turbines

Future developments by MCT include SeaGen turbines to operate like wind turbine farms, in arrays, typically divided into 25MW or 30MW modules. These projects are already in the process of design and development. In April 2015, MCT's tidal turbine designs were attained by Atlantis resources, an Australian corporation working in the marine industry. (Institution of Mechanical Engineers 2018) The designs from MCT's intellectual property portfolio consisted of a next generation 1MW fully submerged SeaGen turbine, designed for floating deployment applications. Also included in the deal the 1.2MW original SeaGen turbine operating for more than five years located on the coast of Northern Ireland. (Institution of Mechanical Engineers 2018)

2.2.3 Atlantis Resources

Atlantis Resources is a firm in Australia that began based on tidal turbine concepts. In 2002 Atlantis started scale models leading onto the deployment of their first 100 kW device installed approximately 50 km south of Melbourne. This device was called the AR1000. With the use of advanced and extensive computer simulations, an enhanced 150 kW turbine was installed and connected to the national grid. The AR1500 was bought about after many years of development. The table below displays the main design features of the three-bladed AR1500 HATT. (SIMEC Atlantis Energy 2015)

Table 3 - AR1500 HATT design parameters (SIMEC Atlantis Energy 2015)

Parameters	
Blade length	9 m
Rotor Diameter	18 m
Rated Power	1.5MW @ 3 m/s
Turbine weight	150 tones
Lifetime	25 years

Currently an AR1500 has been deployed and is operating at MeyGen in the Pentland Firth. MeyGen is a commercially operating tidal stream turbine array consisting of four turbines in total, one of which is an AR1500.



Figure 5 - Atlantis Resources AR1500

2.2.4 Open Hydro

Open hydro, A HATT that designed with open-centre technology, was formed in 2004. The technology was created by Irish American, Herbert Williams in the United States. In 2006 Open hydro became the first large tidal stream device that was deployed at the European Energy Marine Centre (EMEC) and connected to the Scottish grid by 2008, Open Hydro is the first tidal stream turbine in Scotland to deliver electricity to the national grid. (Gov.je, 2019) A 1MW full-scale turbine was then installed in the Bay of Fundy, Canada in 2010. (Gov.je, 2019)

Open Hydro comprises distinctive features to other tidal turbine designs, such as:

- A shaped duct which improves the hydrodynamic efficiency of the rotor. (Lynn 2013)
- A large-diameter permanent-magnet generator is contained within the duct.
- Marine life can pass safely through the open centre.
- A slow-moving rotor with shielded blade tips further reduces risks to marine life.

Table 4 – Open Hydro design parameters (Gov.je, 2019) (Lynn 2013)

Parameters	
Rotor Diameter	16 m
Rated Power	2 MW
Turbine weight	300 tones
Lifetime	25 years

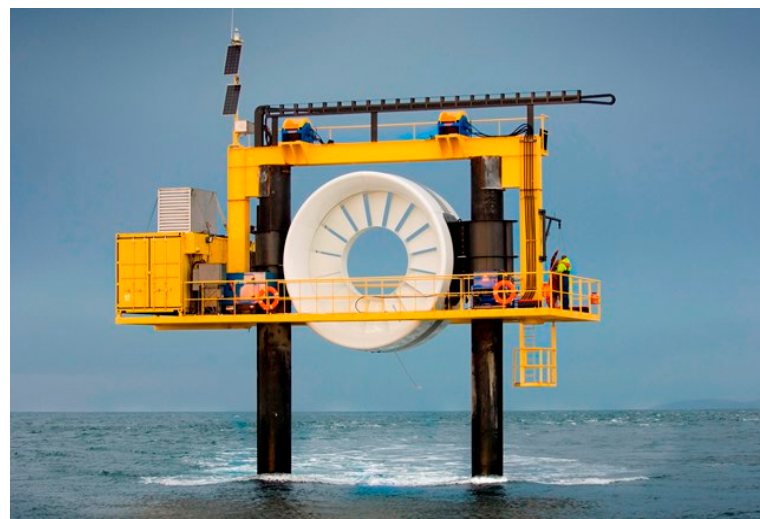


Figure 6 - Open Hydro (Lynn 2013)

2.2.5 Orbital Marine Power Limited

Orbital Marine Power Limited formerly known as Scotrenewables Tidal Power, was founded by offshore engineer Barry Johnston in 2002 in Orkney, Scotland. The company was founded on the basis of developing viably economic floating tidal stream turbines. (ORBITAL MARINE POWER 2018) In 2011, The Company launched the first large scale floating turbine in the world, the SR250, with a power output of 250 kW. This prototype was developed after many years of testing and large investment contributions. After 2.5 years of testing, the turbine produced successful outcomes and was subsequently connected to the national grid, proving the viability of a floating tidal turbine approach. In 2016 the company release the 2MW SR2000, The world's largest tidal energy converter. The device compromised a unique floating approach consisting of two turbines mounted to a floating platform positioning the turbines in the most advantageous parts of the tidal stream. The floating mechanism is displayed in figure 7. Table 5 displays the unique design parameters exhibited by the SR2000. By 2018 25% of the electricity requirements in Orkney were provided by the SR2000 producing approximately 3,000 MWh of energy output. (ORBITAL MARINE POWER 2018)

Table 5 – SR2000 design parameters

Parameters	
Rotor Diameter	16 m
Swept area	2 x 201 m ²
Rated Power	2 MW
Rated Current Speed	3 m/s
Maximum Rotor Speed	16 rpm

The SR2000 is currently part of the FloTEC project funded by the EU's Horizon 2020 programme. The project aims to demonstrate high levels of reliability and survivability whilst furthering the companies understanding on factors such as installation and operation. (Gov.je, 2019) (ORBITAL MARINE POWER 2018)

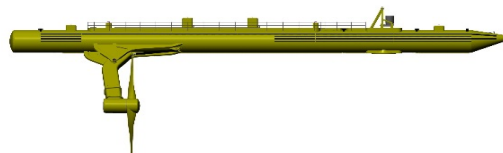


Figure 7 - SR2000 (ORBITAL MARINE POWER 2018)

2.3 Blade design

All of the mentioned companies in this section portray the substantial potential of tidal turbines in the marine industry. Whilst tidal turbines are currently in the infancy stage, factors such as blade design can significantly improve the performance of tidal turbines as a whole.

The potential of a HATT can be increased with an enhanced blade design. The similarities between tidal turbines and wind turbines can be used as an advantage in the case of blade design. Wind turbine blades operate on a spar support structure which can be adapted to the design of a tidal turbine blade. The figure below displays a simple support structure that can be incorporated in a tidal turbine blade.

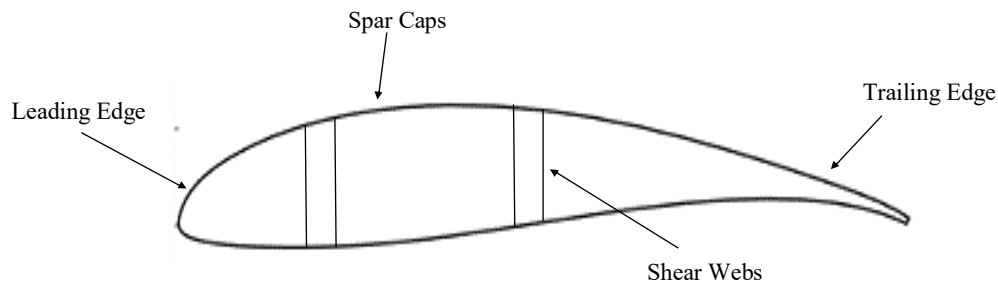


Figure 8 - Spar support structure

The support structure consists of the Leading Edge, Trailing Edge, Spar Caps and Shear Webs. Where the leading edge experiences the highest loading and should therefore comprise of high strength materials. Shear Webs provide structural integrity to the blade.

2.4 Composites

Composite materials are widely used across many industries in today's world. A composite material is a material made of two or more constituent materials. Thus, they offer the prospect of combining materials to give enhanced characteristics. In most cases a composite material consists of fibres and a matrix. Fibres consist of thousands of filaments with diameters between 5 and 15 micrometres. (Gay D, Hoa SV 2003) They exist in the form of either continuous or non-continuous fibres, depending on the application. A matrix is responsible for holding the fibres together and transferring stresses throughout the fibres.

Table 6 displays the common fibre and matrix materials used in a majority of industries. Fibre architecture can be arranged in two ways, unidirectional and woven. Unidirectional fibres run in straight and parallel lines whereas woven architecture consists of groups of fibres called tows that overlap each other perpendicularly. The benefits that unidirectional fibres offer include stiffness and ease in predicting mechanical properties and material strength. Whilst, woven architectures offer the ease of forming complex moulds and better damage tolerance than unidirectional architectures.

Table 6 - Composite Material Comparison

Fibres	Matrix
<i>Glass:</i> <ul style="list-style-type: none">- High strength- Low cost- High impact resistance- Low modulus- Properties degrade after periods of sustained loads	<i>Polymeric:</i> <ul style="list-style-type: none">- Thermoplastic and thermoset resins (epoxies)- Exhibit high mechanical properties
<i>Carbon:</i> <ul style="list-style-type: none">- High specific stiffness and strength- Characterised by different modulus<ul style="list-style-type: none">- High strength <265 GPa- Intermediate Modulus 265-320 GPa- High Modulus 320-440 GPa- Brittle- High cost	<i>Mineral:</i> <ul style="list-style-type: none">- Silicone and Carbon- Useful at high temperature environments
<i>Kevlar:</i> <ul style="list-style-type: none">- Good mechanical properties- High Impact Resistance- Difficult to cut and machine- Susceptible to moisture absorption	<i>Metallic:</i> <ul style="list-style-type: none">- Aluminium alloys- Titanium alloys

2.5 Composite Material Selection

Current wind turbine blades comprise of either Glass Fibre Reinforced polymers (GFRP) or Carbon Fibre Reinforced Polymer (CFRP) and in some cases a mixture of both. Glass fibres are natural materials, thus promote sustainability due to their non-harmful behaviour. (Gay D, Hoa SV 2003) their high strength and corrosion resistance highlight the demand to further research in order to incorporate such composites into tidal turbine applications. Whilst, carbon fibre has substantially low density with a very high strength to weight ratio (Gay D, Hoa SV 2003). After reviewing all possible options for composite materials, GFRP and CFRP were decided as the logical materials to utilise in the design process.

The next step in regard to composite selection involves the identification of a suitable composite layup for the chosen design. The two layups are depicted below, with Layup 1 showing a standard composite layup for a wind turbine blade. Layup 2 however, incorporates a sandwich structure and utilises more plies within each section, specifically the leading edge and spar caps. As a result, Layup 2 has better structural strength and suggests that it is the superior option. Thus, analysis will be developed within the project on both layups to determine the optimal structural layup.

Table 7 - Composite Layup 1

Layup 1	
Leading Edge	45/-45/90/0/90/-45/45
Trailing Edge	45/-45/-45/45
Spar caps	45/-45/0/-45/45
Shear Webs	45/-45/45/-45

Table 8 - Composite Layup 2

Layup 2	
Leading Edge	45/-45/90/0/0/90/-45/45
Trailing Edge	45/-45/0/-45/45
Spar caps	45/-45/90/0/0/90/-45/45
Shear Webs	45/-45/-45/45

Figure 9 below visualises a tidal turbine blade manufactured at NREL, Colorado, from carbon fibre composite. The blade was produced from a mould of the Wortmann FX63 blade and the subsequent model highlights the potential of using carbon fibre in modern tidal turbine applications.

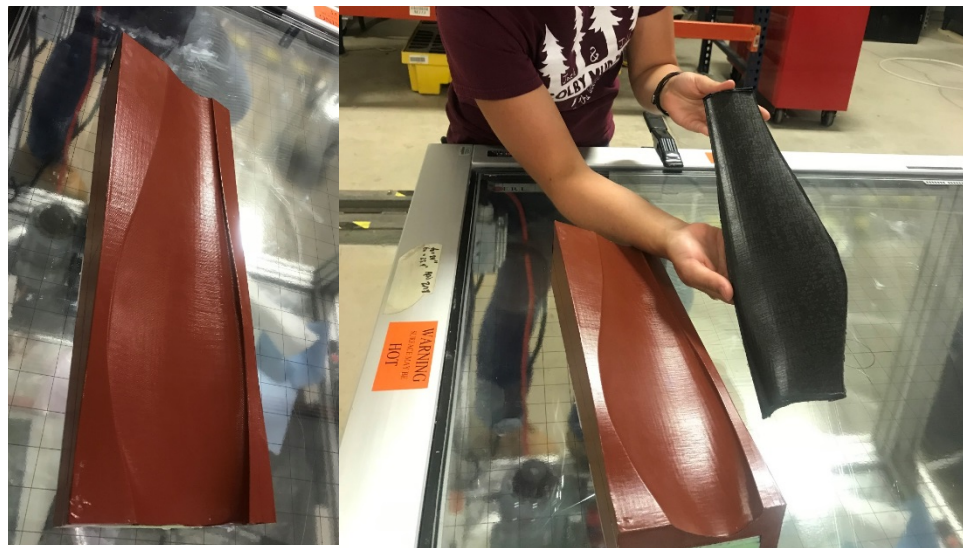


Figure 9 – Example of carbon fibre tidal turbine blade (2018)

2.6 Composite failure criteria

Composite materials require specific failure criteria in order to understand the chance of failure in a material due to the applied loads. For this project the selected failure criteria are:

Tsai-Wu Failure: Tsai- Wu failure criterion is one of the most common existing failure criterions for anisotropic composite materials that have different strengths in tension and compression.

Maximum Stress Failure: Maximum stress failure is failure due to inter-ply stresses causing failure to a structure

Inverse Reverse factor (IRF) was used as a measure for these failure criterions. The safety factor of a structure is the load at which failure occurs divided by the applied load. Therefore, failure occurs when the safety factor is less than 1. The IRF is the reciprocal of the safety factor, therefore the failure of a structure will occur when IRF is greater than 1.

3 METHODOLOGY

The focus of this research was the study and subsequent optimisation of tidal turbine blades. This was done to improve the overall performance of a tidal turbine. Hence, the following design process focused solely on the improvement of one of the turbine blades.

3.1 Design specifications

The Blade design process first initiated with the desired design specifications. These specifications were used to outline the overall design process. These considerations were chosen on the basis of previous research on the optimisation of the blade of a tidal turbine. The design specifications chosen are explained below.

Generally due to the size of tidal turbines, the weight of turbine blades tends to be big. This is a current issue in the marine industry especially in circumstances such as the mobility and installation of a tidal turbine; for this reason, weight reduction is an imperative design specification.

Whilst decreasing the weight of the turbine blade, strength must also be taken into consideration, especially due to the harsh hydrodynamic loads applied to the blade. A balance between blade weight and strength must be placed to guarantee durability.

3.2 Solid Works

CMERG, Cardiff University has been using the Wortmann FX63-137 aerofoil to create the blade geometry shown in figure 6 below. (Ellis et al. 2018) The Wortmann profile shown in Figure 10 was chosen as it comprises high lift characteristics and low stall.

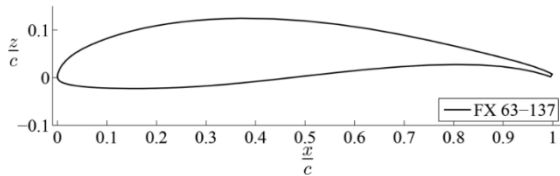


Figure 10 - Wortmann FX63-137 aerofoil (Ellis et al. 2018)

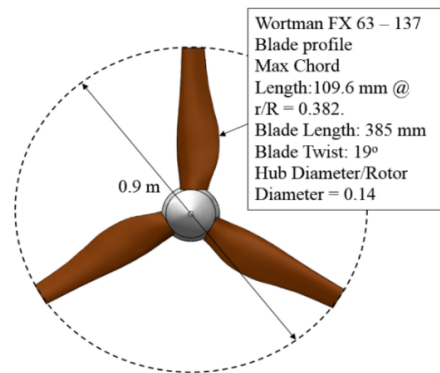


Figure 11 - Turbine rotor (Ellis et al. 2018)

Figure 11 illustrates the Turbine rotor which consists of three blades and a hub, where each blade measures 384.5 mm in length from root to tip, and a hub with a diameter of 130 mm, which in turn allowed for a 0.5 mm gap between the hub and the base of a blade. The overall rotor diameter is 900 mm. (Ellis et al. 2018)

The symmetrical nature of the three blades led to an approximation of basing this project on the sole analysis of a singular blade, as displayed in Figure 12. The solid blade geometry was in the form of a Solid Works file that was altered throughout the optimisation process in this project.



Figure 12 - Blade Geometry (Ellis et al. 2018)

3.3 Finite Element Analysis

The blade geometry was modelled using Finite Element Analysis; A method of predicting and simulating the physical behaviour of complex engineering systems. (Madenci and Guven 2015) The chosen software to model the blade was ANSYS®. Ansys obtains its approximations by decomposing a domain in to a finite number of subdomains, known as elements, for which a systematic solution is constructed by applying vibrational or weighted residual methods. (Madenci and Guven 2015) A solution is obtained through multiple steps; these steps are explained below.

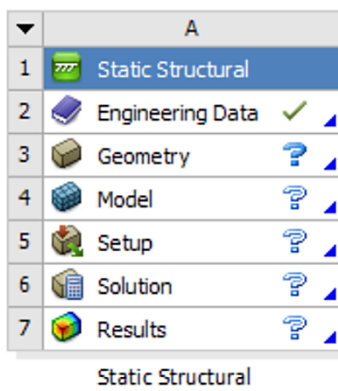


Figure 13 - Ansys Workbench, Static Structural

Figure 13 displays a static structural cell in ANSYS workbench which splits up the simulation process in multiple steps. As seen above, the first step to creating a solution is clarifying the engineering data. The engineering data section contains a selection of different materials, from which the desired material should be determined.

The next step is attaching the geometry that is to be analysed. In this case the geometry that was used is specified in section 3.2.

Following this, the model can now be setup. The model setup includes creating a mesh to mimic a geometry. As mentioned earlier, the mesh is used to subdivide a geometry into subdomains known as elements. A mesh is created by specifying certain parameters in the dialog box that

will define the mesh density. Creating the most appropriate mesh is the basis to any engineering problem, therefore mesh criteria should be studied and inputted correctly.

Once the correct mesh is generated, the model is ready to be analysed. This analysis setup involves the application of loads to the structure whilst defining the appropriate supports. For this project, the loadings, as mentioned in section 3.4, were considered as pressures extracted from previous CFD data. This extraction is done by using a connection between CFX results and static structural in workbench, which is shown in Figure 14.

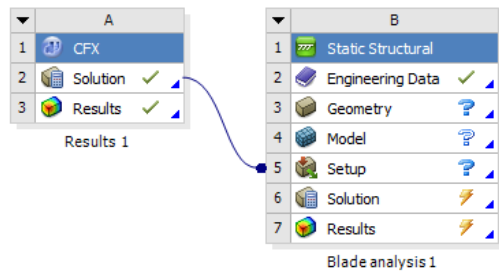


Figure 14 - CFD pressure extraction

The constraint used is a fixed support applied at the blade root to simulate its attachment to the turbine hub. This leads on to the final section of choosing the final solutions of the model, such as the total deformation of the blade.

Once the solutions are received, the results can be analysed and studied, allowing decisions to be made on future changes to the model.

3.3.1 Modelling Composite Materials

Further into the project, ANSYS was used to model a blade made of composite materials. Due to the complexity of modelling composites, ANSYS offers an analysis system called ACP (Pre-Post). This software allows a geometry to be modelled as a layered composite structure.

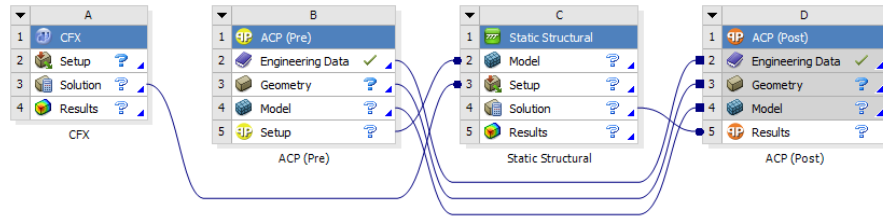


Figure 16 - Composite Material process in ANSYS Workbench

3.3.1.1 ACP (Pre)

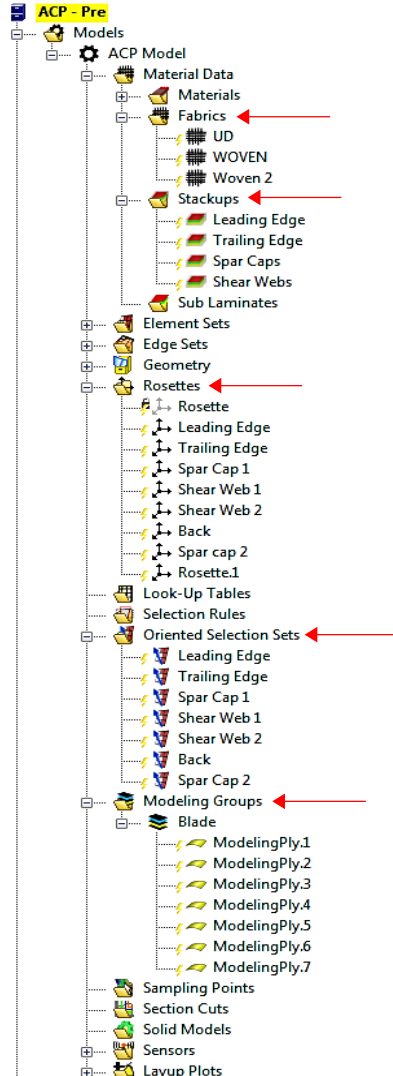


Figure 17 - ACP Toolbar

ACP (Pre) uses definitions such as; number of layers, layer orientation, material and thicknesses to define a composite structure. Once the correct information is inputted, ACP uses this information to generate plies. These plies are imported into the static structural analysis system, shown in Figure 16, and the geometry is analysed as described earlier in this section.

The main definitions required to generate plies in ACP (Pre) are illustrated with red arrows as shown Figure 17 which depicts a tree outline of the simulation process. These definitions are further explained below in the context of this current project:

Fabrics: This section requires the input of the composite materials desired to model the blade. In the case of this project, the desired materials, as specified

in section 2.5, are Epoxy Carbon UD (230 GPa) Prepreg and Epoxy E-Glass UD. This dialog box also required the user to specify a certain thickness, which defines the ply thickness.

Stackups: The integrity of a composite can be significantly enhanced by the layup orientation of each ply; the purpose of this dialog box is defining the number of plies and their corresponding orientations. An example of this is shown in Figure 18.

Rosettes: Rosettes are coordinate systems used to set the Reference Direction of Oriented Selection Sets. (ANSYS Inc. 2013)

Oriented Selection Sets: The Orientated Selection sets are responsible for setting the stacking direction of the associated lay-up. (ANSYS Inc. 2013)

Modeling Groups: Modeling Groups define composite lay-ups. This is ultimately the last step to the ply generation process.

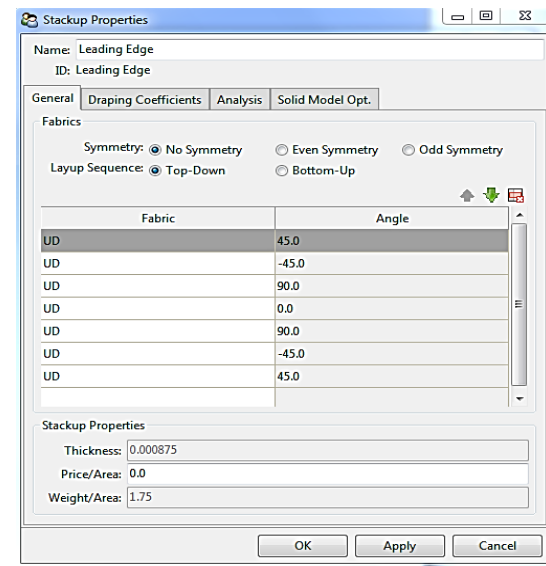


Figure 18 - Stackups dialog box

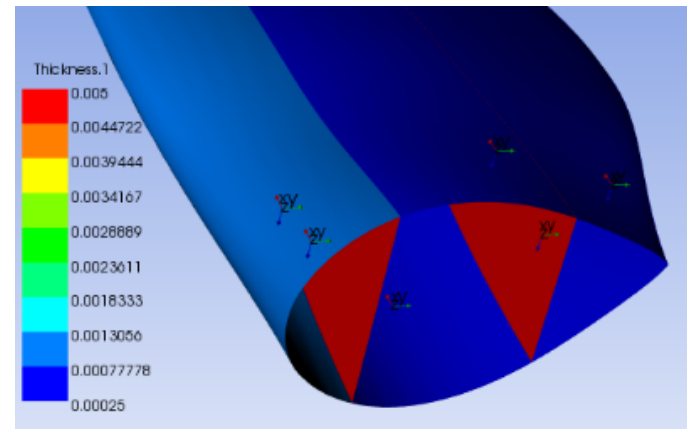


Figure 19 - Generated Ply thicknesses

Figure 19 displays shell thicknesses as a result of the ACP composite layup process. Once the composite structure was defined, it was analysed in the static structural analysis system as demonstrated previously in this section.

3.3.1.2 ACP (Post)

ACP (Post) is a post processing analysis system. It uses results from Static structural to conduct a Failure analysis simulation using the specified failure criteria in section 2.6.

The failure criteria chosen in the dialog box is shown in Figure 20 with the corresponding failure analysis results.

The figure below displays the final outlook to the design process in ANSYS workbench.

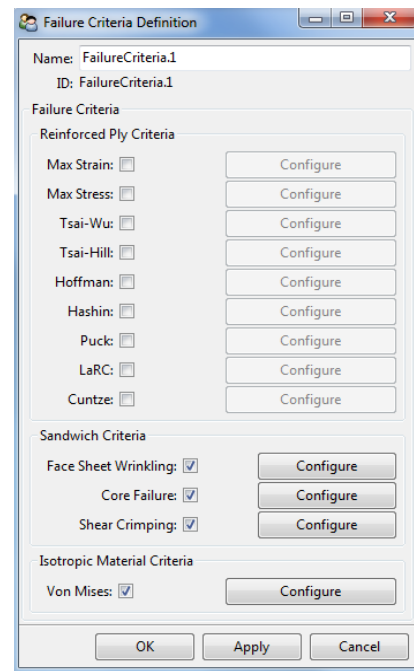


Figure 20 - Failure criteria dialog box

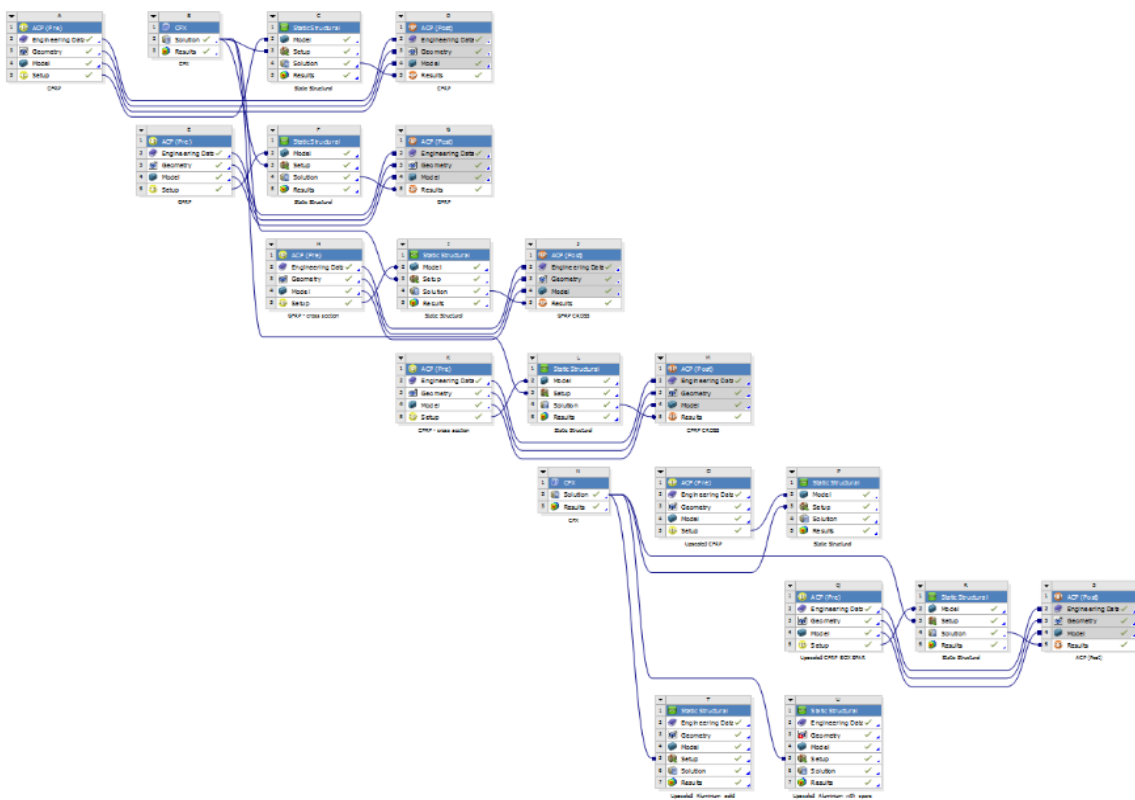


Figure 21 - Final blade analysis process in ANSYS workbench

3.4 CFD data

Results from previous Computational Fluid Dynamics (CFD) were used to simulate the loads exerted by the sea environment onto the blade geometry. Pressures were extracted from the results files and used as blade loadings. The figure below illustrates the pressure distributions across the turbine rotor.

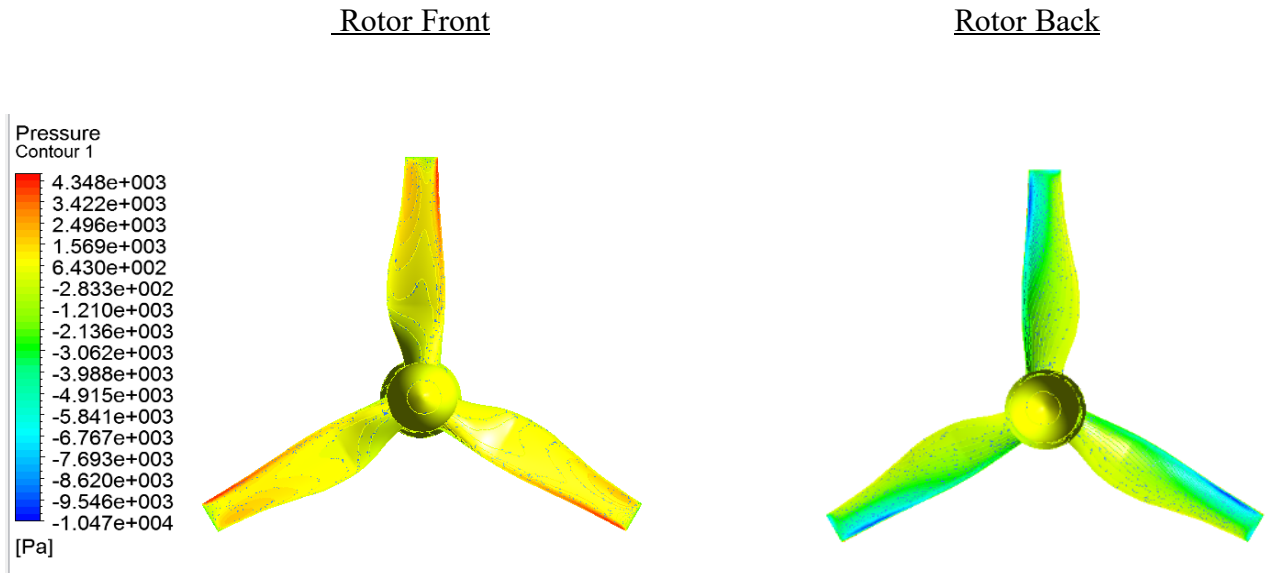


Figure 23 - CFD Pressure distributions

The maximum pressure exerted onto the blade geometry specified in section 3.2, was interpreted to be approximately 4381.5 Pa. Further along the project timeline, an upscaled turbine rotor was analysed. New CFD results were used, corresponding to the upscaled turbine. The maximum pressure exerted on the upscaled blade was approximately 26153.1 Pa.

3.5 Mesh Generation

3.5.1 Mesh sensitivity study

To ensure that the blade was modelled accurately, a mesh sensitivity study was conducted. Before analysing any structure, a mesh sensitivity study should be conducted to ensure that accurate results are received from a simulation, whilst also keeping simulation time to a minimum. The mesh sensitivity study involved applying pressures to a blade geometry and subsequently measuring the deformation of the blade. This iterative process was applied to different meshes structures. The results are shown in the figure below.

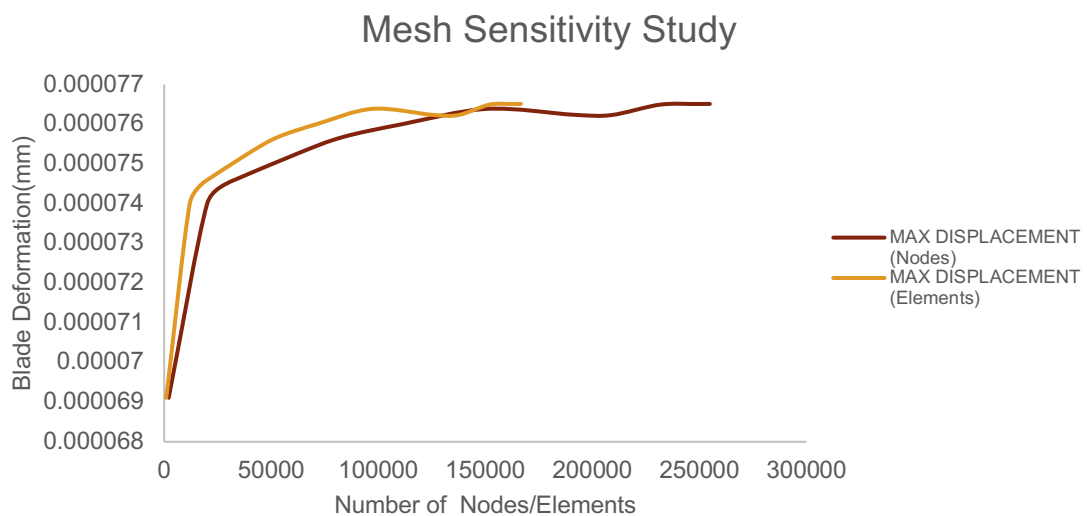


Figure 24 - Mesh Sensitivity study results (No. of Nodes against Deformation of blade)

As depicted in Figure 24, the rate of change in blade deformation after a certain point starts to decrease as the number of elements/nodes increases. This concluded that any increase in the number of elements would not significantly change the results received from a simulation. The chosen number of elements was used as a reference for all future simulations. Details of the chosen mesh can be found in Table 9.

Table 9 - Mesh sensitivity study results

Parameters	Mesh
Number of Elements	166582
Number of Nodes	254833

3.5.2 Mesh details

A suitable mesh was constructed based of the results from the mesh sensitivity study. Certain parameters were defined to ensure the mesh was created correctly. The following table displays details concerning the parameters used to construct the mesh.

Table 10 - Mesh details

Sizing	
Size Function	Proximity and Curvature
Relevance Centre	Course
Max Face Size	4 mm
Max Tet size	4 mm
Min Size	1.5 mm
Proximity Min size	1.5 mm
Transition	Slow
Quality	
Smoothing	High
Average Element Quality Mesh Metric	0.82589
Average Skewness Mesh Metric	0.24437

A suitable mesh can be deduced in various ways. According to (Sharcnet [no date]) (ANSYS [no date]), the generated mesh was considered suitable due to the following reasons:

- The Average Skewness Mesh Metric lay in the range of $> 0 — 0.25$ deducing an “excellent” cell quality
- An Average Element Quality Mesh Metric of value 1 indicates a perfect cube or square, therefore the average mesh metric received deduced a good element quality

Figure 25 illustrates the generated mesh for the first blade simulation.

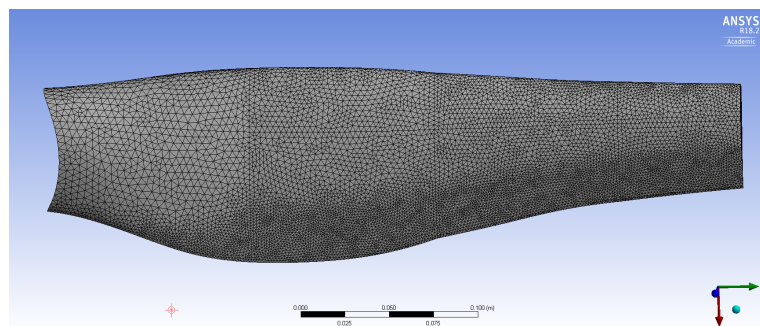


Figure 25 - Generated blade mesh

3.5.3 Composite blade mesh details

ACP (Pre) requires a shell geometry when building any composite model. As a result, the geometry is modelled using shell elements compromising an internal support structure. This results in different mesh settings to the original solid blade. The following table shows the mesh details for the shell blade.

Table 11 - Composite blade mesh details

Sizing	
Size Function	Proximity and Curvature
Relevance Centre	Fine
Max Face Size	6 mm
Min Size	0.5 mm
Proximity Min size	0.5 mm
Quality	
Smoothing	High
Average Element Quality Mesh Metric	0.94924
Average Skewness Mesh Metric	0.056378

This mesh was achieved by applying extra settings such as:

- A body sizing of 1 mm across the whole blade
- An edge sizing of 0.5 mm on the trailing edge
- An Automatic method, setting the face mesh type to quadrilaterals.

As mentioned in the previous section, the generated mesh is considered to be high quality as it exhibits an “excellent” cell quality shown from the Average Skewness Mesh Metric. The Average Element Quality Mesh Metric indicates the face mesh to be close to a perfect square. The generated mesh for the composite blade is illustrated in the figure below.

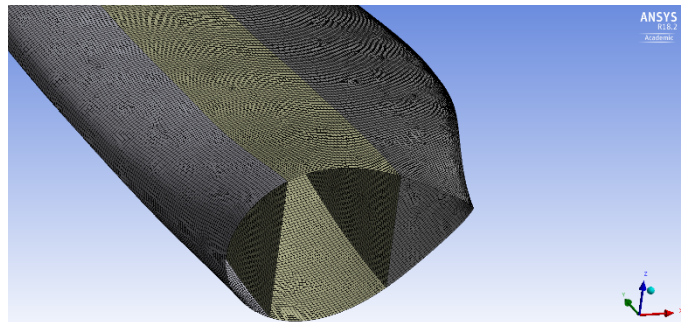


Figure 26 - Composite blade Mesh

3.6 Blade Design Process

Multiple steps were included in this project to receive a final blade model. The design process is illustrated in the Figure 26 as seen below:

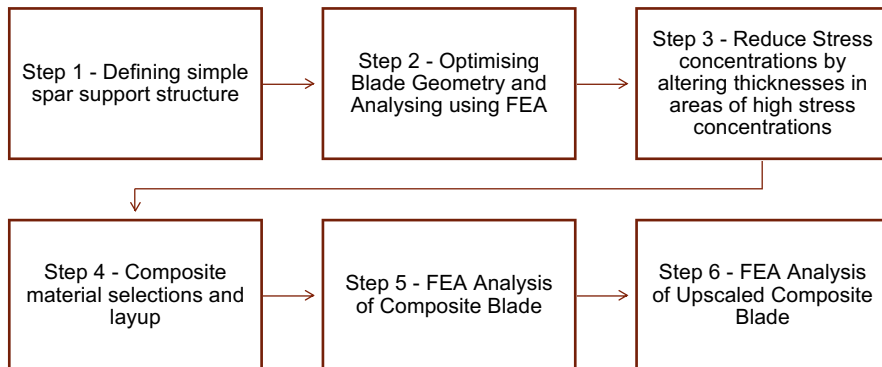


Figure 27 - Flow chart of design process

4 RESULTS & DISCUSSION

The performance of the blade was measured by various factors such as; the Total Deformation and the Equivalent (Von Mises) Stress experienced in the blade. In this project the total deformation ultimately represented the tip deflection of the blade. The Equivalent (Von Mises) Stress allows any arbitrary three-dimensional stress state to be represented as a single positive stress value (SAS IP [no date]). These factors were considered alongside overall weight reduction in order to meet the design criteria mentioned in section 4.1. In the following sections the particular factors will be illustrated with the Total Deformation on the left and the Equivalent (Von Mises) Stress on the right-hand side of the page.

The safety factor across the blade was also measured when required. ANSYS provides a stress tool which is based off the maximum equivalent stress failure theory for ductile materials, such as aluminium. (Fluent 2015) The safety factor is ultimately the yield stress of the selected material divided by the maximum equivalent stress exhibited by the structure. This factor is useful when looking at failure due to maximum equivalent stress. Therefore, a stress factor less than 1 indicates failure of the structure.

4.1 Aluminium blade

4.1.1 Solid Blade

The geometry specified in section 4.3 was first modelled as a solid aluminium blade. This simulation was used as a reference point to all forthcoming simulations. The total deformation of the blade was found to be 0.22 mm. The blade also exhibited a maximum stress of 2.78 MPa. Considering the yield stress of aluminium to be 280 MPa, it was deduced that this blade was strong enough to withstand high loads. The total deformation and maximum stress are displayed below in Figure 28.

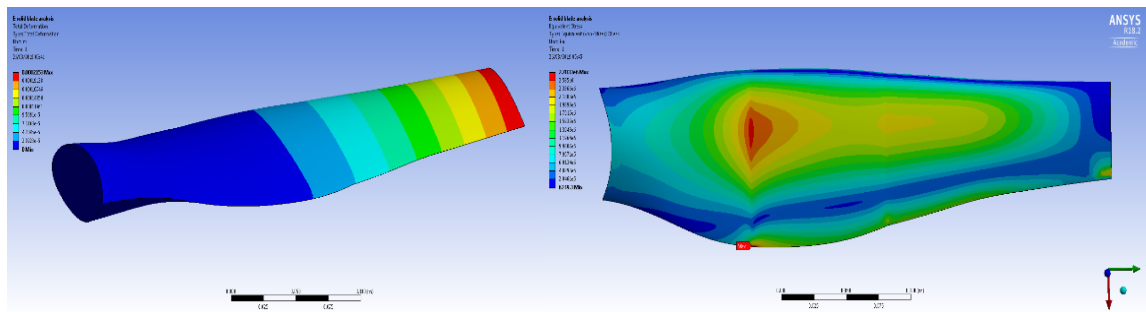


Figure 28 - Solid Blade

However, the mass of the blade was 1.04 kg. The next blade iterations focused on the reducing this value whilst upholding the blades ultimate strength.

4.1.2 Hollow Blade

For this reason, the next simulation involved the development of a “worst-case” scenario blade, which is a completely hollow aluminium blade with no internal support structure. The figure below shows a total deformation of 2.87 mm and a maximum stress of 119 MPa.

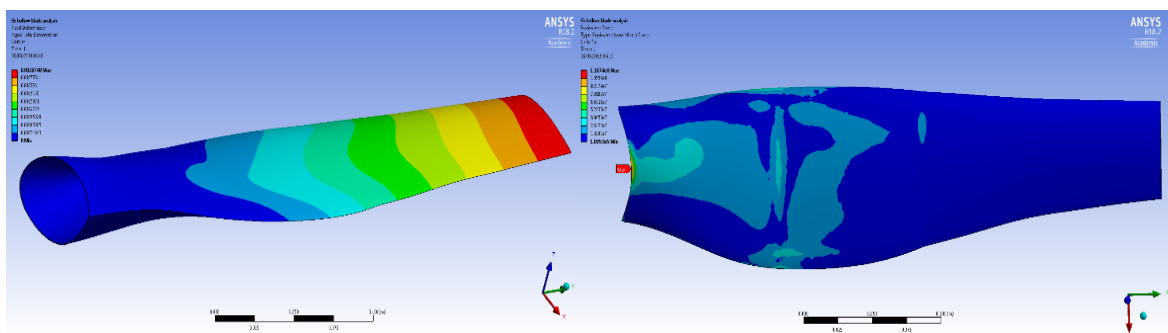


Figure 29 - Hollow blade

This value of maximum stress interpreted for this blade was significantly high and edging towards the yield stress of aluminium. This led to extra evaluation by looking at the safety factor across the blade.

Figure 30 displays the various safety factor values across the blade. As shown in the legend, the blue regions denote regions with a safety factor of 15, whereas the red regions indicate a safety factor of 0, where failure occurs.

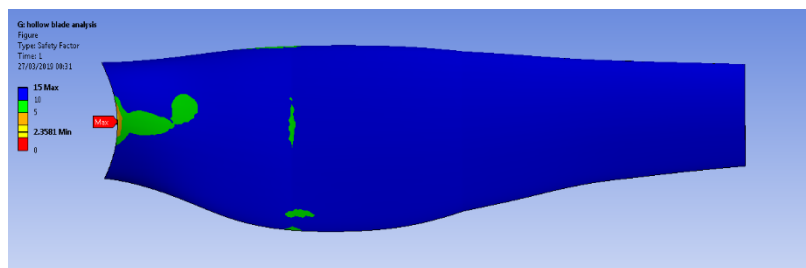


Figure 30 - Safety factor for hollow blade

The minimum safety factor on the blade visualised by the yellow/orange regions has a value of 2.4 inferring that the blade will not fail. However, fatigue can eventually result in failure after loading the blade over multiple cycles. The resulting weight of this blade was 0.07 kg, deducing a 93% weight reduction from the solid aluminium blade.

4.1.3 Optimised blade

With the use of blade calculations, a simple support structure was formed. After iteratively modelling the structure on ANSYS, an optimised internal support structure was produced. The cross-sectional area of the blade is shown in Figure 31.

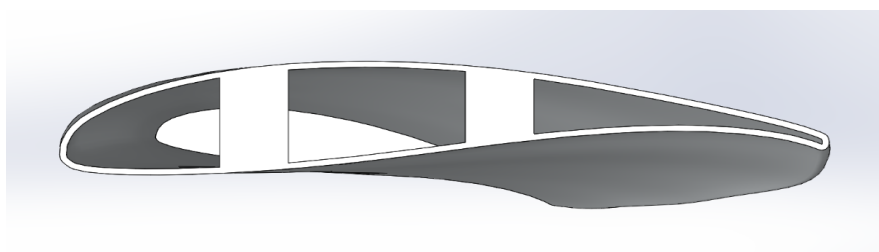


Figure 31 - Cross section view of spar support structure

The internal support structure consisted of shear webs, with thickness of 1 mm. The blade exhibited high ultimate strength and decreased tip deflection, as shown in Figure 42. The blade exhibited a total deformation of 0.26 mm and a maximum stress of 5.24 MPa. The resulting mass of the blade was 0.49 kg showing a percentage decrease of 52% from the original blade.

A safety factor of 15 was apprehended from this blade, deducing a suitable blade structure.

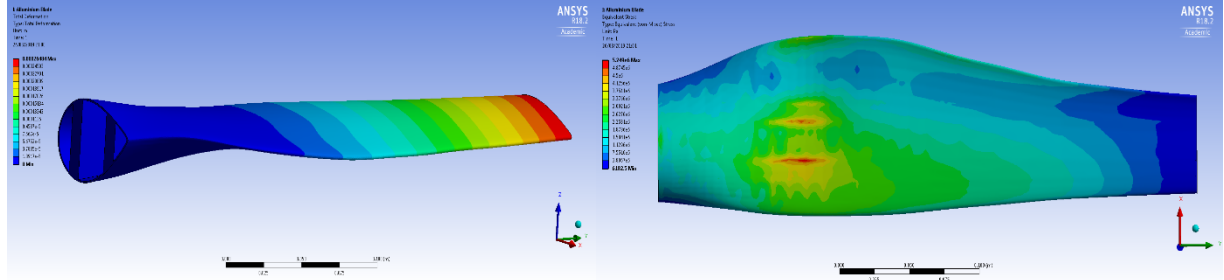


Figure 32 -Aluminium blade with spars

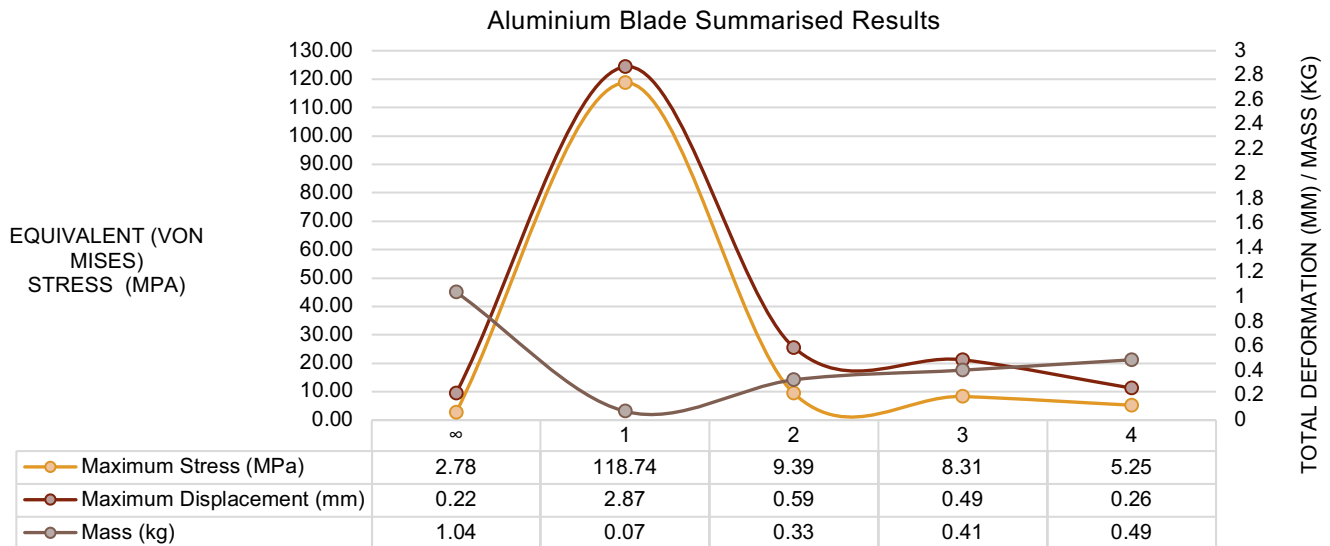


Figure 33 - Summarised Aluminium blade results

Figure 33 displays the summarised results of the iterative design process shown throughout this section. As mentioned previously the solid blade aluminium was used as a reference point and is denoted by ∞ . The “worst case” scenario hollow aluminium blade is indicated with the value 1. Clearly visualised on the graph the total deformation and maximum stress exhibited by blade 1 is significantly larger than the other blades. Blades 2, 3 and 4 represent the iterative process of reaching the final optimised blade, blade 4.

4.2 Composite blade optimisation

The next stage of this project involved the composite optimisation of the blade. CFRP and GFRP were the chosen materials used to model the blade as mentioned in section 2.5.

4.2.1 CFRP Blade

Using the layup 1 specified in section 2.5 the blade was modelled as a CFRP blade. The first blade consisted of an internal support structure with shear webs of thickness 1 mm. Figure 34 displays the CFRP blade with a total deformation of 0.27 mm and a maximum stress of 5.68 MPa.

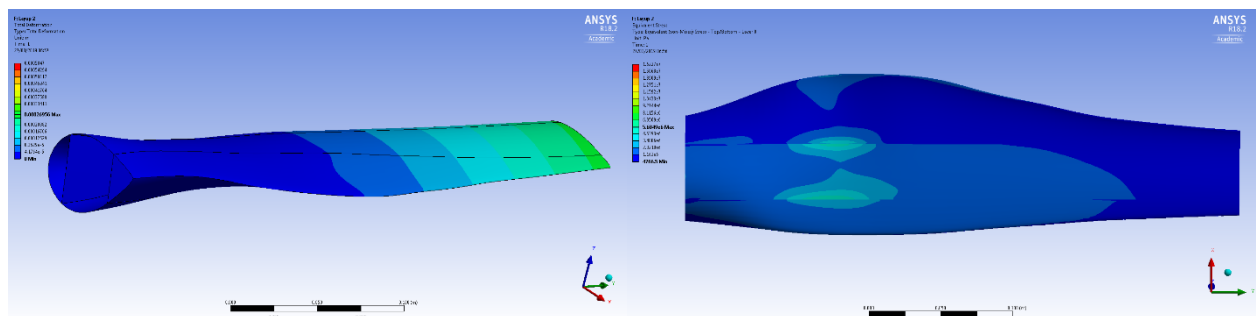


Figure 34 - CFRP blade (1 mm Shear Webs)

The mass of this blade was 0.31 kg. This demonstrated significant improvement to the aluminium blade mentioned in the previous section, as the CFRP exhibited a 37% mass reduction to the aluminium blade whilst upholding similar total deformation and maximum stress values. This led onto the decision of modelling the CFRP blade with 0.5 mm shear webs.

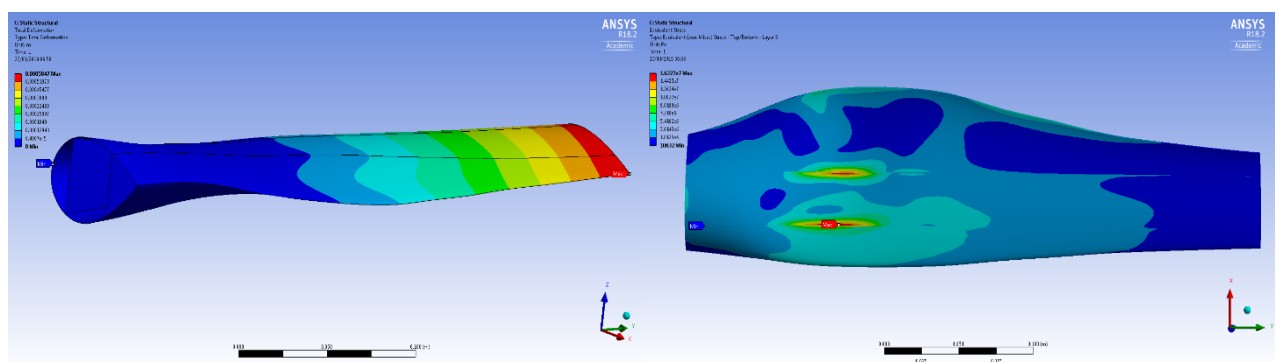


Figure 35 - CFRP blade (0.5 mm Shear Webs)

Figure 35 shows an increase in both total deformation and maximum stress, with values of 0.58 mm and 16.2 MPa respectively. The figure clearly illustrates the increase in stress concentrations at the shear webs. The increase in maximum stress and total deformation appeared viable as the mass of the blade was 0.14 kg achieving a 55% decrease in mass to the 1 mm CFRP blade. The IRF value for this blade was 0.032 for both failure criterions deducing that the blade would not fail as the IRF value is significantly less than 1.

4.2.2 GFRP Blade

The blade was then analysed with the same layup as GFRP blade. The blade exhibited a total deformation of 1.96 mm and a maximum stress of 17.1 MPa whilst having a mass of 0.2 kg.

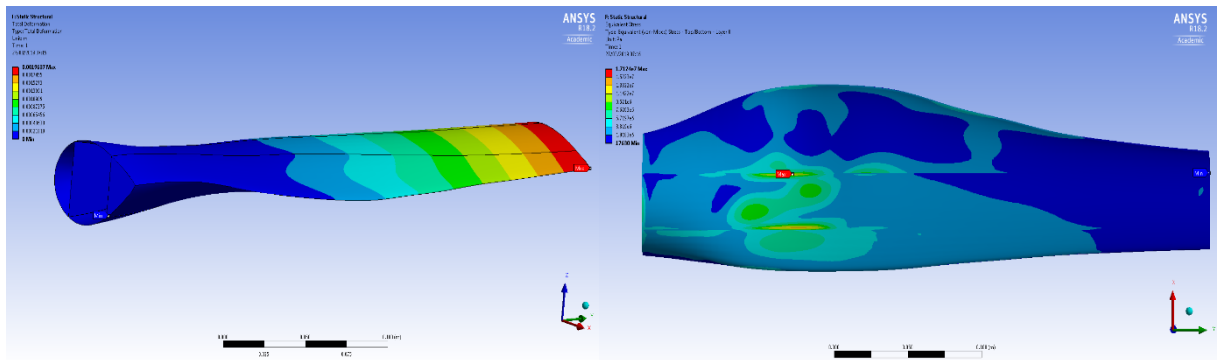


Figure 36 - GFRP (0.5 mm Shear Webs)

The IRF for the Tsai- Wu and the maximum stress criterion were 0.152 and 0.167 respectively deducing that the blade would not face failure. However, these values are almost five times greater than the ones of the CFRP blade, subsequently reducing the margins of safety.

Different spar structures were analysed using both CFRP and GFRP, for example a crossed web design was adapted as shown in the Figure 37.

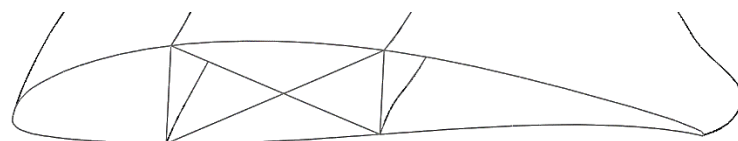


Figure 37- Cross beam spar support structure

This design was analysed but resulted in minor improvements to the original composite blades. As shown in the figure below the IRF value for the Tsai –Wu criterion has marginally decreased.

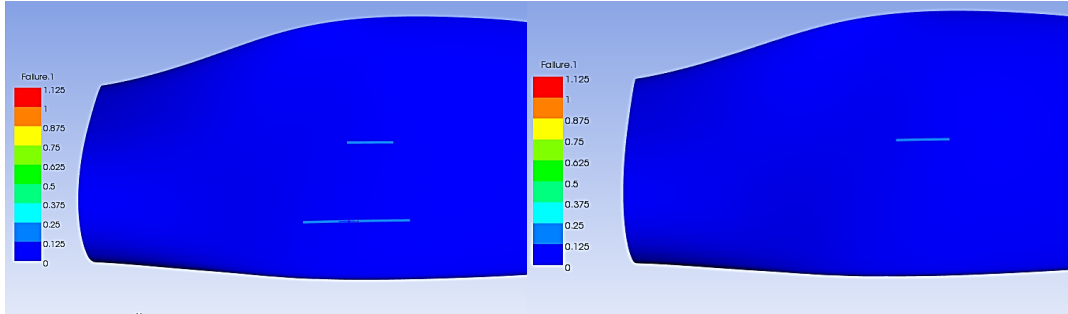


Figure 38 - Tsai- Wu comparison between GFRP (left) and GFRP cross webs (right)

Figure 39 below displays the comparison between the various CFRP and GFRP blades. The graph shows a significant increase in deformation, maximum stress and mass between the original CFRP blade and the adapted cross webs design CFRP blade. Although the cross webs design slightly improved these factors for the GFRP blade, the GFRP blade exhibited significantly higher values of total deformation, maximum stress and mass.

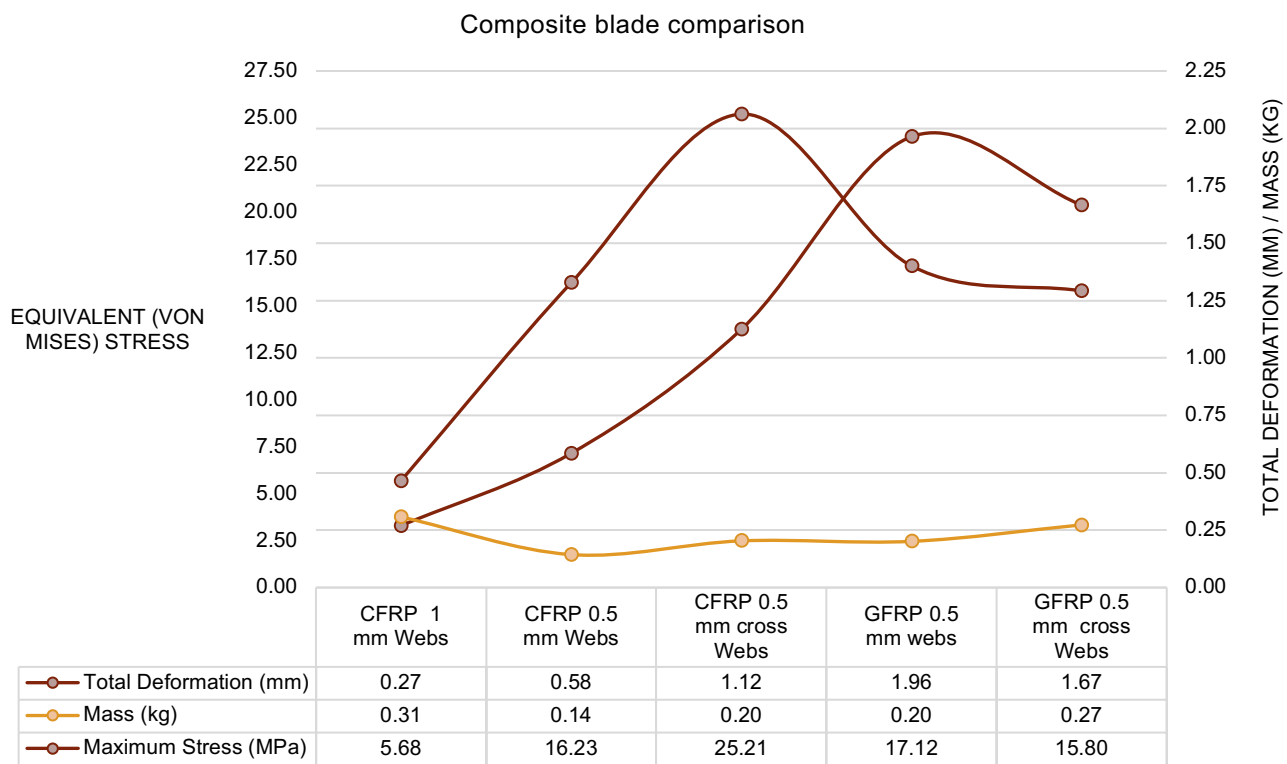


Figure 39 - Composite blade comparison

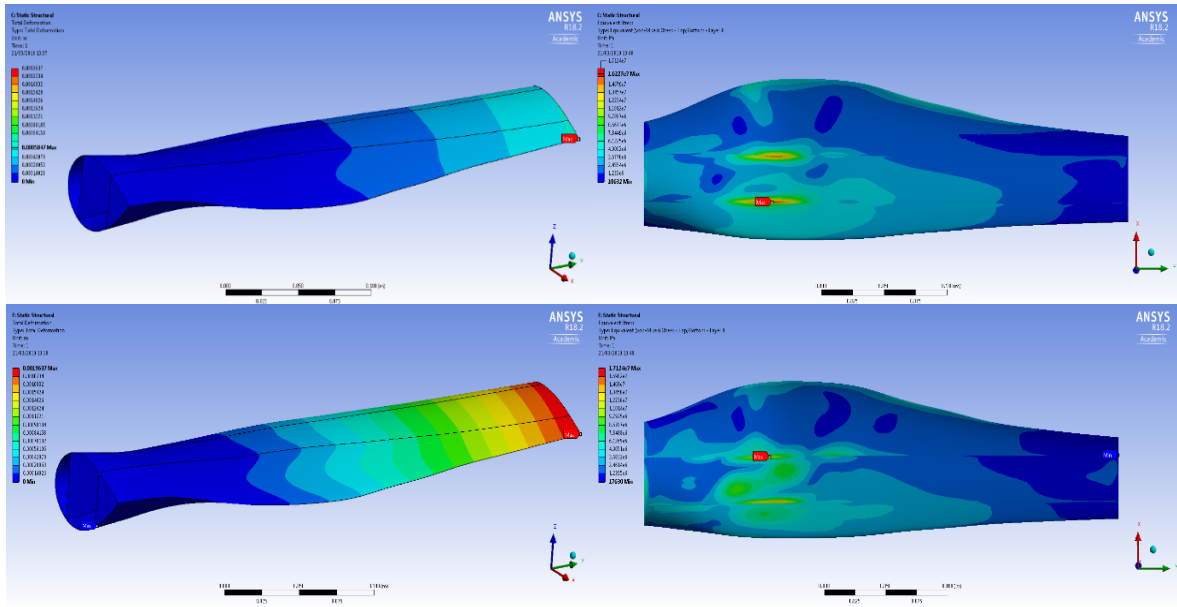


Figure 40 - CFRP (top) vs GFRP (bottom)

Figure 40 visualises the comparison between the CFRP and the GFRP 0.5 mm web blades, clearly favouring the CFRP over the GFRP blades. This conclusion aided in the decision of choosing the CFRP blade to move forward to the next stage of the project.

4.3 Upscaled Blade optimisation

The last stage of this project utilised results from the previous sections to develop the final design. The final design included upscaling the shell model so that the turbine rotor was 10 m in diameter. The previous section deduced the suitability of using CFRP as the final material whereas this section will focus on the different ply layups of the CFRP blade. The upscaled aluminium blades were first analysed and used as a reference point for further simulations.

Table 12 displays the important factors regarding the aluminium blades.

Table 12 - Upscaled Aluminium blades

	Total Deformation (mm)	Maximum Stress (MPa)	Mass (kg)
Upscaled Aluminium blade	10.35	15.1	1468.3
Upscaled Aluminium blade with internal support structure	10.80	21.2	478.31

4.3.1 Composite Layup 1

The first CFRP blade was modelled using layup 1. The total deformation and maximum stress of this blade is 75.20 mm and 181 MPa respectively. With a mass of 185.11 kg. Although the weight is significantly smaller than the aluminium blade, this CFRP blade exhibits a considerably larger deformation and maximum stress. The IRF of Tsai-Wu and Maximum stress for this blade are 0.66 and 0.77 respectively. These values indicate that the blade will not fail however, they are significantly high resulting in a small safety margin.

4.3.2 Composite Layup 2

After many composite layup iterations and various spar support structured designs were developed, A CFRP blade compromising a box spar support structure and a composite layup specified in section 2.5 was deduced. The final blade exhibited a total deformation of 32.87 mm, a maximum stress of 68.9 MPa and a final mass of 265.25 kg. The IRF of Tsai-Wu and Maximum stress for this blade are 0.28 and 0.26 respectively. The figure below displays the comparison between the composite layup 1 and layup 2.

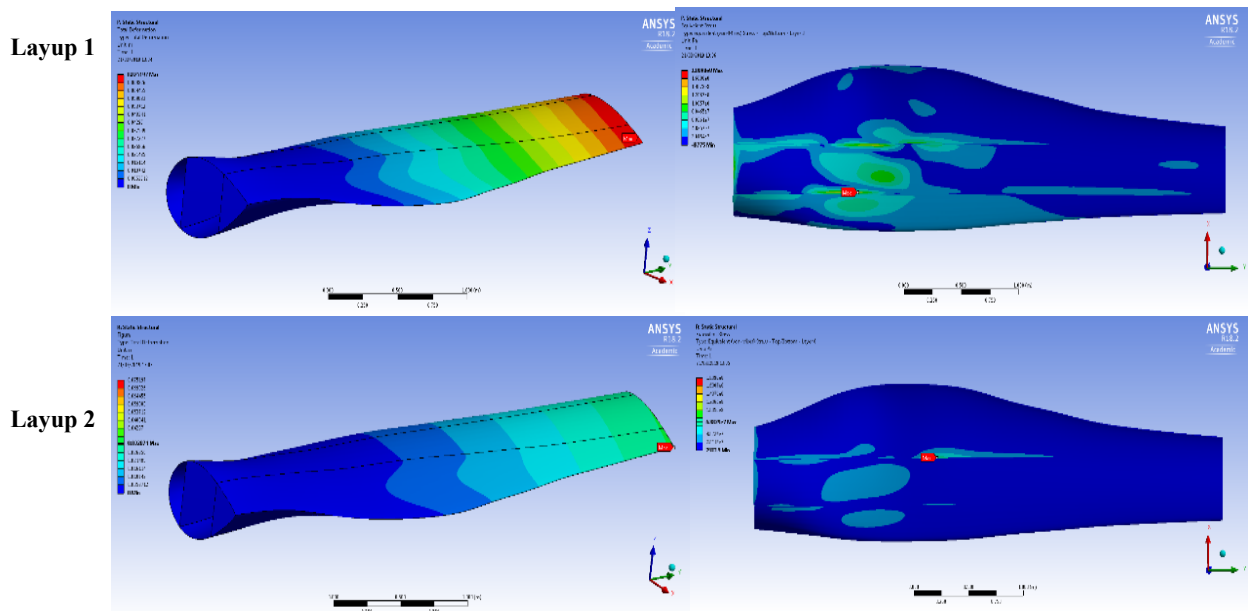


Figure 41 - Comparison between composite layups of CFRP blades

Figure 42 displays the significant difference between the two composite layups, with layup one showing potential failures in multiple areas of the blade. The use of layup 2 not only reduced the margin of safety of the blade but also reduced the areas across the blade that could cause potential failures as illustrated below.

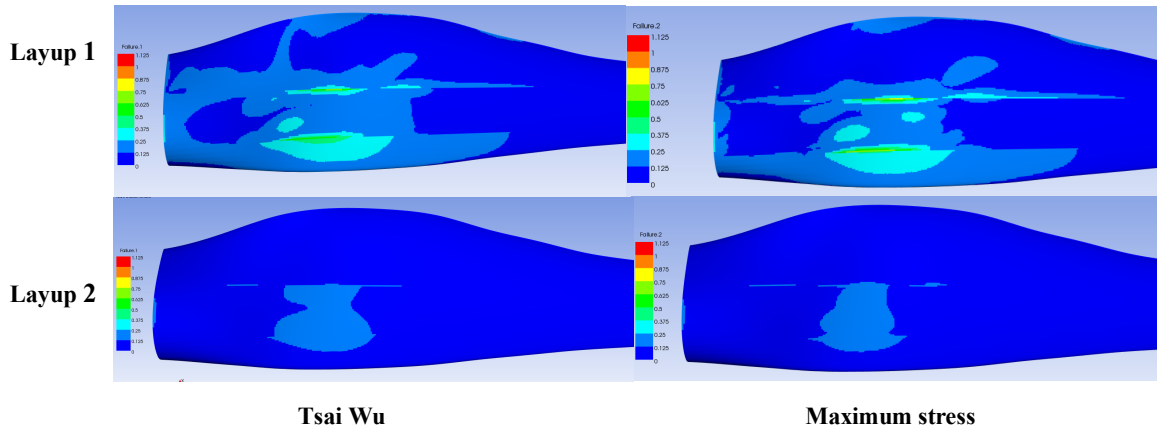


Figure 42 – Failure comparison between the composite layups

Figure 43 illustrates the design process of reaching the final design. It can be seen that the final blade saw an 82% decrease in mass from the initial solid aluminium blade and a 45% mass reduction to the aluminium spar blade whilst exhibiting viable increases in deformations and stresses. The choice of using composite layup 2 is clearly illustrated with the substantial decrease in stresses and deformations in comparison to CFRP composite layup 1. The stresses experienced by the blade were further decreased by incorporating the box spar design.

Although carbon fibre produces optimal results, it should be noted that it has high cost per unit area whilst aluminium is cheap and produces a structurally resilient blade. Thus, the utilisation of carbon fibre is economically restrained and subject to the designer's financial budget. Factors such as weight, durability and cost of production should be thoroughly considered throughout the development and manufacture of tidal turbine technologies.

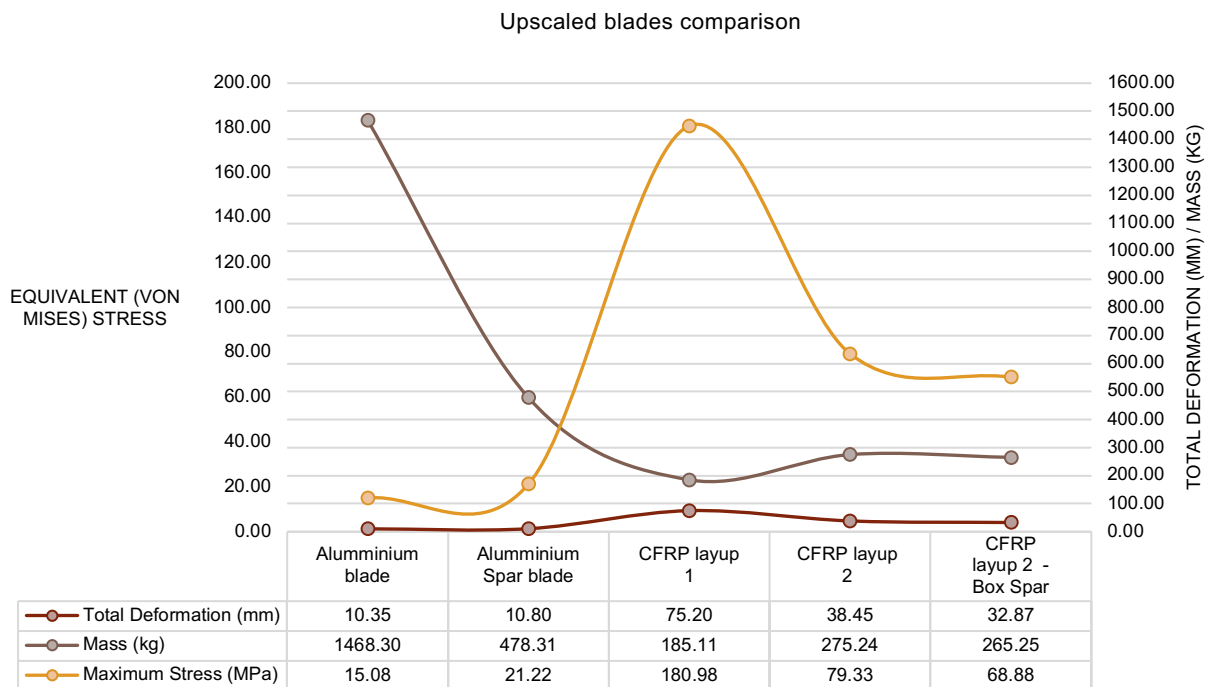


Figure 43 - Upscaled blades comparison

This design process concluded the final design that comprised of a box spar support structure and a composite layup capable of withstanding the hydrodynamic loads exerted by the ocean waters. The figure below illustrates the final mesh and internal structure of the blade.

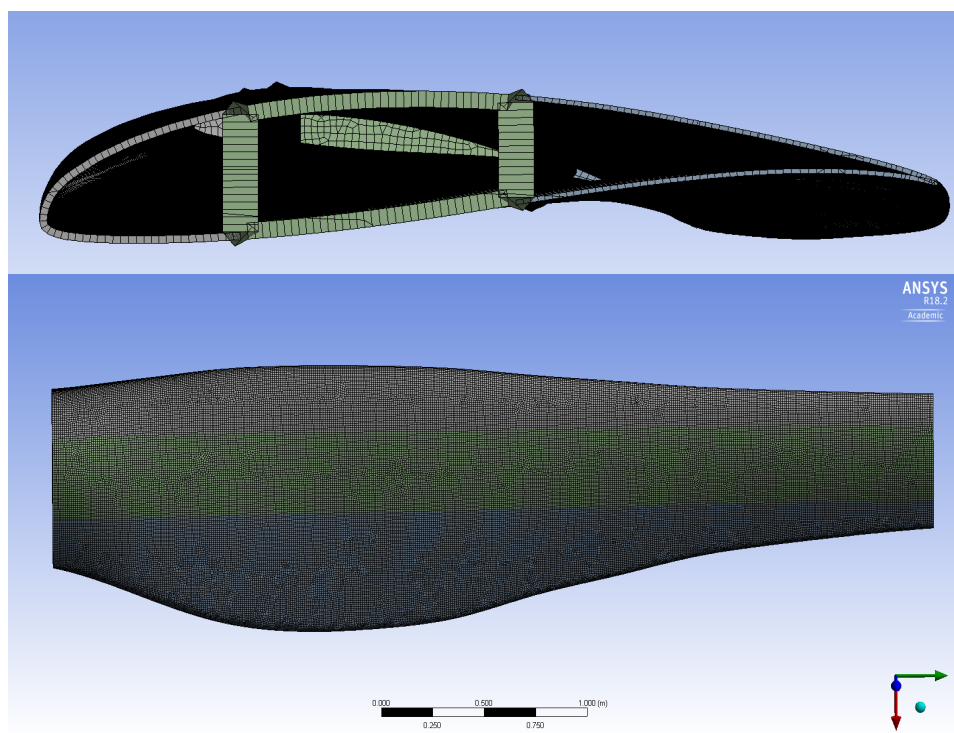


Figure 44 – Final CFRP blade

5 CONCLUSION

The method of Finite element Analysis was used to enhance the internal and composite layup structure of HATT blade. Analysis was conducted on blades made of aluminium, CFRP and GFRP. Blade deformations and equivalent stresses exhibited by the blade provided understanding of the blade structure, allowing design modifications to be made correspondingly. Alongside these factors, failure criteria were chosen and used to deduce the suitability of the choice of composite material and layup orientation throughout the blade. In Concern to this project multiple conclusions were made including:

- An internal support structure can be adapted for the purposes of maximum weight reduction in a tidal turbine blade.
- A box spar support structure design offered maximum integrity and strength to the tidal turbine blade.
- CFRP was found to be the most suitable material for the design of the blade. Providing minimal deformations and stress concentrations when compared to a GFRP blade.
- The composite layup deduced from the design process demonstrated high strength and minimal deformations in comparison to the initial composite layup.
- The final composite layup resulted in increased safety margins and fewer areas across the blade exposed to the possibility of failure across the blade.
- The final design comprising of a box spar support structure and the selected composite layup deduced an 82% weight reduction compared to the original solid aluminium blade whilst exhibiting a marginally viable increase in total deformation and maximum stress.

For the purposes of this project it can be concluded that the resulting model met the objectives of this project by comprising both composite materials and a spar support structure producing a mesh capable of withstanding the hydrodynamic loading exerted by the marine environment.

Throughout the duration of this project, a few issues arose. These issues included the difficulty of developing a suitable surface mesh due to the licencing limits of the utilised programme constraining the number of allowable elements and nodes in a model. Difficulties also arose when modelling the blade using composite materials due to the lack of experience with finite element modelling of composites.

Future Work

Composite Layups: As seen from section 5.2.3, the tip deflection and strength of the blade were significantly improved solely due to the change of composite layup. The further study of composite layup and ply orientations can be altered to enhance the structural properties of a turbine blade.

Transient modelling: Transient modelling of the tidal turbine blade can be a future consideration in order to receive greater understanding on the impacts of inertial forces on the tidal turbine blade

Fluid Structural Interaction Modelling (FSI): FSI modelling provides further understanding of the coupling interaction between structures and fluids, this can be useful in the future when studying the progressive impact of the water onto the blades.

Fatigue due to resonance: Whilst the turbine is operating the blades will experience constant resonance eventually causing damage after a long period of time. Studying fatigue due to resonance can aid in forming an improved support structure capable of resisting any damage caused by resonance.

6 REFERENCES

- ANSYS [no date]. Element quality mesh analysis. Available at:
https://www.sharcnet.ca/Software/Ansys/16.2.3/en-us/help/wb_msh/msh_Element_Quality_Metric.html [Accessed: 2 March 2019].
- ANSYS Inc. 2013. ANSYS Composite PrepPost User's Guide. *ANSYS Manual* 15317(November), pp. 724–746. Available at:
https://www.academia.edu/25099111/ANSYS_Composite_PrepPost_Users_Guide.
- BP 2018. *2018 BP Energy Outlook 2018 BP Energy Outlook*. Available at:
<https://www.bp.com/content/dam/bp/business-sites/en/global/corporate/pdfs/energy-economics/energy-outlook/bp-energy-outlook-2018.pdf>.
- Chauhan, P. et al. 2015. Tidal Stream Turbine-Introduction, current and future Tidal power stations. *National Conference on Innovative and Emerging Technologies (NCIET-2015)* (April). doi: 10.13140/RG.2.1.1823.2489.
- Ellis, R. et al. 2018. Design process for a scale horizontal axis tidal turbine blade. In: *Proceedings of the 4th Asian Wave and Tidal Energy Conference*., pp. 1–8.
- European Marine Energy Centre 2013. European Marine Energy Centre. Available at: <http://www.emec.org.uk/about-us/our-tidal-clients/open-hydro/>.
- Fisher, S. et al. 2018. Tidal Stream Industry Update. (February). Available at: www.itpenergised.com.
- Fluent 2015. *ANSYS FLUENT User 's Guide*. Available at: <http://ccpbbscm-1.central.cranfield.ac.uk/ansys/v162/readme.html>.
- Fraenkel, P.L. 2007. Marine current turbines: Pioneering the development of marine kinetic energy converters. *Proceedings of the Institution of Mechanical Engineers, Part A: Journal of Power and Energy* 221(2), pp. 159–169. Available at: <http://journals.sagepub.com/doi/10.1243/09576509JPE307>.
- Gay D, Hoa SV, T.S. 2003. *Composite materials design and applications*. CRC Press. Available at: <https://epdf.tips/composite-materials-design-and-applications.html>.
- Gnos, P. 2013. *ANDRITZ HYDRO Hammerfest Developer and supplier of turnkey tidal power arrays*. Available at: <http://www.andritzhydrohammerfest.co.uk/> [Accessed: 20 February 2019].
- Hardisty, J. (Jack) 2009. *The analysis of tidal stream power*. Wiley.
- Huckerby, J., Jeffrey, H., Sedgwick, J., Jay, B. and Finlay, L. 2012. An international vision for Ocean energy- version II. *Ocean Energy Systems Implementing Agreement* . Available at: <http://www.powerprojects.co.nz/files/pictures/International Vision>

Brochure V2.pdf.

- Institution of Mechanical Engineers 2015. Atlantis buys Marine Current Turbines. Available at: <http://www.imeche.org/news/news-article/atlantis-buys-marine-current-turbines-29041502>.
- Jenkins, N. and Ekanayake, J. 2018. *Renewable Energy Engineering*. Cambridge University Press. Available at:
<https://www.cambridge.org/core/product/identifier/9781139236256/type/book>.
- Lloyd, C. et al. 2019. Analysis of a Horizontal-Axis Tidal Turbine Performance in the Presence of Regular and Irregular Waves Using Two Control Strategies. *Energies* 12(3), p. 367. doi: 10.3390/en12030367.
- Lynn, P.A. 2013. *Electricity from Wave and Tide*. Available at:
<https://www.wiley.com/en-us/Electricity+from+Wave+and+Tide%3A+An+Introduction+to+Marine+Energy-p-9781118340912>.
- Madenci, E. and Guven, I. 2015. *The finite element method and applications in engineering using ANSYS®, second edition*. Boston, MA: Springer US. Available at: <http://link.springer.com/10.1007/978-0-387-28290-9>.
- Marsh, G. 2004. Tidal turbines harness the power of the sea. *Reinforced Plastics* 48(6), pp. 44–47. Available at:
<https://www.sciencedirect.com/science/article/pii/S0034361704003443>.
- MCT 2012. SeaGen-S 2MW The SeaGen Advantage. Available at:
<https://www.atlantisresourcesltd.com/wp/wp-content/uploads/2016/08/SeaGen-Brochure.pdf>.
- MCT 2013. Marine Current Turbines™: Seaflow., pp. 1–10. Available at: www.marineturbines.com.
- ORBITAL MARINE POWER 2018. Orbital Marine Power - the world leader in the development of floating tidal stream and run-of-river turbines. Available at: <https://orbitalmarine.com/technology-development/orbital-o2>.
- Rourke, F.O. et al. 2010. Tidal energy update 2009. *Applied Energy* 87(2), pp. 398–409. Available at: <https://linkinghub.elsevier.com/retrieve/pii/S030626190900347X>.
- SAS IP, I. [no date]. Equivalent (von Mises). Available at:
https://www.sharcnet.ca/Software/Ansys/17.0/en-us/help/wb_sim/ds_Equiv_Stress.html [Accessed: 14 March 2019].
- Sharcnet [no date]. Skewness. Available at:

https://www.sharcnet.ca/Software/Ansys/17.0/en-us/help/wb_msh/msh_skewness.html.

- SIMEC Atlantis Energy 2015. *AR1500 Tidal Turbine*. Available at: <https://www.atlantisresourcesltd.com/wp/wp-content/uploads/2016/08/AR1500-Brochure-Final-1.pdf>.
- Uihlein, A. and Magagna, D. 2016. Wave and tidal current energy - A review of the current state of research beyond technology. *Renewable and Sustainable Energy Reviews* 58, pp. 1070–1081. Available at: <http://dx.doi.org/10.1016/j.rser.2015.12.284>

7 APPENDICES

7.1 Raw Data

Table 13 – Modal Results from Blade Simulations

	Total deformation (mm)	Maximum stress (MPa)	Mass (kg)
Solid Aluminium Blade	0.19	2.47	1.07
Aluminium blade 1 mm Webs	0.26	5.25	0.49
CFRP 1 mm Webs	0.27	5.68	0.31
CFRP 0.5 mm Webs	0.58	16.23	0.14
CFRP 0.5 mm cross Webs	1.12	25.21	0.20
GFRP 0.5 mm webs	1.96	17.12	0.20
GFRP 0.5 mm cross webs	1.67	15.80	0.27
Aluminium Blade	10.35	15.08	1468.30
Aluminium Spar Blade	10.80	21.22	478.31
CFRP Layup 1	75.20	180.98	185.11
CFRP Layup 2	38.45	79.33	275.24
CFRP Layup 2 - Box Spar	32.87	68.88	265.25

Table 14 - Inverse Reserve factors of Failure Criteria for Composite Blades

Inverse Reserve factors				
	Tsai-Wu		Max stress	
	Min	Max	Min	Max
CFRP	0.0002	0.032	0.0002	0.032
GFRP	0.0001	0.152	0.0001	0.167
CFRP cross	0.0001	0.09	0.0001	0.12
GFRP cross	0.0001	0.148	0.00008	0.163
Upscaled CFRP layup 1	0.002	0.66	0.002	0.77
Upscaled CFRP layup 2	0.0002	0.28	0.0002	0.26

7.2 Record of meetings

Appendix A – Record of project meetings

CARDIFF SCHOOL OF ENGINEERING

NAME.. Miriam Said STUDENT NUMBER..... 1673667

SUPERVISOR... Dr. Tim O'Doherty, Dr. Allan Mason Jones

TEACHING DISCIPLINE MMM

Date of meeting	Supervisor's assessment of progress	Actions by next meeting	Supervisor signature
9 /10 /18	Starting to look at modelling	Research on subject area	L. Mair
16 /10 /18	"	"	L. Mair
23 /10 /18	"	GANTT CHART PPP	L. Mair
30 /10 /18	Starting develop model	Geometric and making	L. Mair
6 /11 /18	"	"	L. Mair
13 /11 /18	"	"	L. Mair
20 /11 /18	"	"	L. Mair
27 /11 /18	"	"	L. Mair
4 /12 /18	"	"	L. Mair
11 /12 /18	"	"	L. Mair
31 /12 /18	"	"	L. Mair
7 /01 /19	"	"	L. Mair

(Copy this sheet if necessary for additional meetings; it is also available on Blackboard as a Word document)

Appendix A – Record of project meetings

CARDIFF SCHOOL OF ENGINEERING

NAME.....Mimam STUDENT NUMBER.....1673667.....

SUPERVISOR.....Pr. Tim O'Doherty, Pr. Allan-Mason-Sones

TEACHING DISCIPLINEMM.....

Date of meeting	Supervisor's assessment of progress	Actions by next meeting	Supervisor signature
14 / 02/19	Start to finalise Results and Comp	Show some further plotting to continue	L.Mason
21 / 02/19	"	"	L.Mason
28 / 02/19	"	"	L.Mason
7 / 03/19	looking computer	assess if enough time to model	L.Mason
14 / 03/19	Put report together	Show progress of report	L.Mason
21 / 03 /19	"	"	L.Mason

(Copy this sheet if necessary for additional meetings; it is also available on Blackboard as a Word document)